

MHD Mixed Convection Flow of Casson Fluid over a Moving Wedge Saturated in a Porous Medium in the presence of Chemical Reaction and Convective Boundary Conditions

Imran Ullah^{1*}, Sharidan Shafie¹ and Ilyas Khan²

¹Department of Mathematical Sciences, Faculty of Science, Universiti Teknologi Malaysia, 81310 UTM Johor Bahru, Johor, Malaysia

²College of Engineering, Majmaah University, Majmaah 11952, Saudi Arabia

Received 30 September 2017; accepted 30 November 2017; available online 28 December 2017

Abstract: This work concerned to hydromagnetic mixed convection flow of Casson fluid over a wedge. It is assumed that the wedge is moving inside a porous medium. The effects of chemical reaction, slip and convective boundary conditions at velocity, temperature and concentration walls are also considered. The governing partial differential equations are converted into ordinary differential equations using similarity transformations, and then solved by implicit finite difference scheme. Comparisons with the existing literature are performed and good agreement is achieved. The influence of physical parameters on flow fields are illustrated graphically. It is observed that the velocity rises with the increment in Casson fluid parameter and magnetic parameter. It is also noticed that thickness of thermal boundary layer grows with the increase of radiation. The skin friction coefficient enhances with the increase of porosity parameter while reduces as Casson fluid and moving wedge parameters increase. Increase in heat and mass transfer rate is noticed to be enhanced with the increase in radiation and chemical reaction parameters, respectively.

Keyword: Casson fluid; wedge; MHD; mixed convection; chemical reaction

1. Introduction

There has been a growing interest in the analysis of magnetohydrodynamic (MHD) flow due to many practical applications such as in MHD flowmetry, MHD power generators, MHD pumps, high temperature plasmas, chemical processing equipment, power generation systems and cooling of nuclear reactors. As a consequence, a considerable amount of research has been carried out to have a look at the effects of electrically conducting fluids inclusive of liquid metals, water mixed with a little acid and others under the influence of a magnetic field on the flow and heat transfer aspects in different geometries. The Falkner-Skan wedge problem was extended by Watanabe and Pop [1] to the electrically conducting flow and studied MHD buoyancy driven flow past a wedge. Yih [2] presented numerical solutions of MHD forced convection flow generated by wedge with viscous dissipation. The effects of magnetic field on two dimensional flow of viscous fluid past a wedge under the influence of thermal radiation was developed by Chamkha *et al.* [3]. Ishak *et al.* [4] analyzed

the hydromagnetic flow of micropolar fluid due to wedge with constant surface heat flux. Uddin and Kumar [5] explored the magnetic field influence on electrically conducting flow of micropolar fluid over a wedge. They obtained the similarity solutions for the flow fields and observed that increase in wedge angle enhance the friction factor. On the other hand, the impact of radiation on MHD flow of nanofluid through porous medium in the presence of chemical reaction was investigated by Zhang *et al.* [6]. They observed that the fluid temperature rises with the strength of radiation parameter. Khan *et al.* [7] presented the numerical solutions for hydromagnetic flow of nanofluid over a moving wedge in the presence of viscous dissipation. Pandey and Kumar [8] studied the effects of suction and injection on electrically conducting flow of nanofluid due to wedge with heat generation.

It is well known that MHD mixed convection heat transfer flow in both porous and non-porous medium is of great interest because of its wide range engineering and industrial applications such as high temperature plasmas, drying of porous solid, droplet filters, the cooling of nuclear reactors,

*Corresponding author: ullahimran14@gmail.com
2017 UTHM Publisher. All right reserved.
penerbit.uthm.edu.my/ojs/index.php/jst

pumps, solar power collector and thermal designing of buildings. Aydin and Kaya [9] numerically investigated the radiation effects on MHD mixed convection flow over a porous plate using Keller-box method. Kandasamy *et al.* [10] analyzed the chemical reaction effects on mixed convection flow past a permeable wedge with thermophoresis and magnetic field. The series solutions for electrically conducting mixed convection flow of viscoelastic fluid over a porous wedge was presented by Hsiao [11]. Author noticed that velocity and temperature behave oppositely with the growth of mixed convection parameter. Su *et al.* [12] explored the radiation effects on hydromagnetic mixed convection flow of Newtonian fluid generated by wedge in the presence of ohmic heating. Khan *et al.* [13] described hydromagnetic Falkner-Skan mixed convection flow through porous medium with convective boundary condition. Prasad *et al.* [14] obtained numerical solution of electrically conducting mixed convection flow over a wedge via Keller-box method. Mohammad [15] examined the effects of thermal radiation on mixed convection flow due to wedge saturated in a porous medium in the presence of heat generation and magnetic field. Ravindran *et al.* [16] described chemically reactive mixed convection flow due to vertical cone under the influence of magnetic field.

The study of non-Newtonian fluid has gained ample attention of researchers in the last few decades. The highly nonlinear equations of these fluids present challenge to mathematicians, physicists and engineers due to which their interest in these fluids are increasing day by day. Among several other models, Casson fluid model has attracted several researchers and investigated Casson model with various physical aspects. In particular, at low shear rate the Casson fluid model describes the flow characteristics of blood more precisely and when it flows through small blood vessels. Mukhopadhyay and Mandal [17] investigated the suction and blowing effects on two dimensional flow of Casson fluid over a wedge with variable surface heat flux. Mahanta and Shaw [18] examined three dimensional MHD flow of Casson fluid in a porous medium with convective boundary condition. The influence of magnetic field on mixed convection flow of Casson nanofluid with convective boundary

conditions was described by Imtiaz *et al.* [19]. Raju and Sandeep [20] analyzed MHD flow of Casson fluid due to moving wedge in the presence of slip and viscous dissipation.

In present study, the effect of chemical reaction on MHD mixed convection flow of Casson fluid over a moving wedge with convective boundary conditions is investigated. It is assumed that the wedge is moving in a porous medium. The similarity solutions are obtained numerically via Keller-box method [21]. The effects of physical parameters are obtained and displayed graphically.

2. Mathematical Formulation

The hydromagnetic mixed convection flow of Casson fluid over a moving wedge saturated in porous medium in the presence of magnetic field is considered. It is assumed that wedge is moving with the velocity $u_w(x) = U_w x^m$ and the free stream velocity $u_e(x) = U_\infty x^m$, where U_w and U_∞ are constants. Here $m = \frac{\beta_1}{(2 - \beta_1)}$,

β_1 is the Hartree pressure gradient parameter that corresponds to $\beta_1 = \frac{\Omega}{\pi}$ for the total angle

Ω of the wedge (see Fig. 1). A uniform magnetic field is applied to the wedge surface. The induced magnetic field is neglected due to low magnetic Reynolds number.

The rheological governing equations for momentum and energy are given as

$$\frac{\partial u}{\partial x} + \frac{\partial v}{\partial y} = 0, \tag{1}$$

$$u \frac{\partial u}{\partial x} + v \frac{\partial u}{\partial y} = u_e \frac{\partial u_e}{\partial x} + v \left(1 + \frac{1}{\beta} \right) \frac{\partial^2 u}{\partial y^2} + \frac{\sigma B^2(x)}{\rho_f} (u_e - u) + \left(1 + \frac{1}{\beta} \right) \frac{v \varphi}{k_1} (u_e - u) + [\beta_T (T - T_\infty) + \beta_C (C - C_\infty)] g_x \sin \frac{\Omega}{2}, \tag{2}$$

$$u \frac{\partial T}{\partial x} + v \frac{\partial T}{\partial y} = \alpha \frac{\partial^2 T}{\partial y^2} - \frac{1}{\rho c_p} \frac{\partial q_r}{\partial y}, \tag{3}$$

$$u \frac{\partial C}{\partial x} + v \frac{\partial C}{\partial y} = D_m \frac{\partial^2 C}{\partial y^2} - k_c (C - C_\infty). \tag{4}$$

The corresponding boundary conditions are

$$u = u_w(x) + N_1 v \left(1 + \frac{1}{\beta} \right) \frac{\partial u}{\partial y}, \quad v = 0,$$

$$k \frac{\partial T}{\partial y} = -h_f (T_f - T),$$

$$D_m \frac{\partial C}{\partial y} = -h_s (C_s - C) \text{ at } y=0, \quad (5)$$

$$u \rightarrow u_e(x), T \rightarrow T_\infty, C \rightarrow C_\infty \text{ as } y \rightarrow \infty, \quad (6)$$

where u and v denote the velocity components in x - and y -directions respectively, ν is kinematic viscosity, σ is the electrically conductivity, $B(x) = B_0 x^{(m-1)/2}$ is magnetic field with B_0 is the strength of the magnetic field, ρ is the fluid density, ϕ is the porosity, $k_1(x) = k_0 x^{-(m-1)}$ is the permeability of porous medium, g is the gravitational force due to acceleration, β_T is the volumetric coefficient of thermal expansion T is the fluid temperature, β is the Casson parameter,

$\alpha = \frac{\kappa}{\rho c_p}$ is the thermal diffusivity of the

Casson fluid, κ is the thermal conductivity of fluid, c_p is the specific heat at constant pressure, q_r is the radiative heat flux, D_m is the mass diffusivity, $k_c(x) = ak_2 x^{m-1}$ is the variable rate of chemical reaction k_2 is a constant reaction rate and a is the reference

length along the flow., $N_1(x) = N_0 x^{\frac{m-1}{2}}$ denotes velocity slip factor with constant N_0 ,

$h_f(x) = h_0 x^{\frac{m-1}{2}}$ and $h_s(x) = h_1 x^{\frac{m-1}{2}}$ represents

the convective heat and mass transfer with h_0 ,

h_1 as constants, $T_f(x) = T_\infty + T_0 x^{2m-1}$ in which T_0 being reference temperature and

$C_s(x) = C_\infty + C_0 x^{2m-1}$ with C_0 being reference concentration.

Making use of Rosseland approximation for radiation, the radiative heat flux q_r is introduced as

$$q_r = \frac{-4\sigma^*}{3k_1^*} \frac{\partial T^4}{\partial y} \quad (7)$$

where σ^* is the Stefan-Boltzmann constant and k_1^* is the mean absorption coefficient. We can express T^4 as linear function of temperature. It is derived by expanding T^4 in a Taylor series about T_∞ and neglecting higher terms, one can write

$$T^4 \cong 4T_\infty^3 T - 3T_\infty^4. \quad (8)$$

Incorporating Eqs. (7) and (8) in Eq. (3), can be written as

$$u \frac{\partial T}{\partial x} + v \frac{\partial T}{\partial y} = \alpha \frac{\partial^2 T}{\partial y^2} + \frac{16\sigma^* T_\infty^3}{3\rho c_p k_1^*} \frac{\partial^2 T}{\partial y^2} \quad (9)$$

Introducing the following similarity transformations

$$\psi = \sqrt{\frac{2\nu x u_e}{m+1}} f(\eta), \quad \eta = \sqrt{\frac{(m+1)u_e}{2\nu}} y, \quad \theta = \frac{T - T_\infty}{T_f - T_\infty},$$

$$\phi = \frac{C - C_\infty}{C_s - C_\infty} \quad (10)$$

where the stream function ψ is defined by the following relations

$$u = \frac{\partial \psi}{\partial y}, \quad v = -\frac{\partial \psi}{\partial x} \quad (11)$$

and satisfies the continuity equation given in Eq. (1).

From Eqs. (2-9), non-dimensional system of equation will take the following form

$$\left(1 + \frac{1}{\beta}\right) f''' + ff'' + \frac{2m}{m+1}(1-f'^2) + \frac{2M}{m+1}(1-f') + \frac{2}{m+1}\left(1 + \frac{1}{\beta}\right)K(1-f') + \frac{2}{m+1}(Gr\theta + Gm\phi)\sin\left(\frac{2m}{m+1}\frac{\pi}{2}\right), \quad (12)$$

$$\frac{1}{Pr}\left(1 + \frac{4}{3}R_d\right)\theta'' + f\theta' - \frac{2(2m-1)}{m+1}f'\theta = 0, \quad (13)$$

$$\frac{1}{Sc}\phi'' + f\phi' - \frac{2(2m-1)}{m+1}f'\phi - \frac{2}{m+1}R\phi = 0. \quad (14)$$

The transformed boundary conditions are

$$f(0) = 0, f'(0) = \gamma + \delta\sqrt{\frac{m+1}{2}}\left(1 + \frac{1}{\beta}\right)f''(0),$$

$$\theta'(0) = -\left(\sqrt{\frac{2}{m+1}}\right)Bi_1[1 - \theta(0)],$$

$$\phi'(0) = -\left(\sqrt{\frac{2}{m+1}}\right)Bi_2[1 - \phi(0)], \quad (15)$$

$$f'(\infty) = 1, \theta(\infty) = 0, \phi(\infty) = 0, \quad (16)$$

$$\text{where } M = \frac{\sigma B_0^2}{\rho_f U_\infty}, K = \frac{\nu\phi}{k_0 U_\infty}, Gr = \frac{g_x \beta_T T_0}{U_\infty^2},$$

$$Gm = \frac{g_x \beta_C C_0}{U_\infty^2}, Pr = \frac{\nu}{\alpha}, R_d = \frac{4\sigma^* T_\infty^3}{kk_1^*}, Sc = \frac{\nu}{D},$$

$$R = \frac{2\nu k_2}{(m+1)U_\infty}, \gamma = \frac{U_w}{U_\infty}, \delta = N_0\sqrt{U_\infty\nu},$$

$$Bi_1 = \frac{h_0}{k} \left[\frac{\nu}{U_\infty} \right]^{1/2}, Bi_2 = \frac{h_1}{D_m} \left[\frac{\nu}{U_\infty} \right]^{1/2}.$$

are magnetic parameter, porosity parameter, thermal Grashof number, mass Grashof number, Prandtl number, radiation parameter, Schmidt number, chemical reaction parameter, moving wedge parameter, slip parameter and Biot numbers.

Expressions for physical quantities of interest in present problem are skin friction coefficient Cf_x , Nusselt number Nu_x and Sherwood number Sh_x which are defined by:

$$Cf_x = \frac{\tau_w}{\rho u_e^2}, Nu_x = \frac{xq_w}{\alpha(T_f - T_\infty)},$$

$$Sh_x = \frac{xq_s}{D_m(C_s - C_\infty)}, \quad (16)$$

where τ_w , q_w and q_s are the wall skin friction, wall heat flux and wall mass flux, respectively, defined by

$$\tau_w = \mu_B \left(1 + \frac{1}{\beta} \right) \left[\frac{\partial u}{\partial y} \right]_{y=0},$$

$$q_w = - \left(\left(\alpha + \frac{16\sigma^* T_\infty^3}{3\rho c_p k_1} \right) \frac{\partial T}{\partial y} \right)_{y=0},$$

$$q_s = -D \left(\frac{\partial C}{\partial y} \right)_{y=0} \quad (17)$$

Using Eq. (10) in Eq. (17), the non-dimensional skin friction coefficient, Nusselt number and Sherwood number can be written as

$$(Re_x)^{1/2} Cf_x = \sqrt{\frac{m+1}{2}} \left(1 + \frac{1}{\beta} \right) f''(0),$$

$$(Re_x)^{-1/2} Nu_x = -\sqrt{\frac{m+1}{2}} \left(1 + \frac{4}{3} R_d \right) \theta'(0),$$

$$(Re_x)^{-1/2} Sh_x = -\sqrt{\frac{m+1}{2}} \phi'(0) \quad (18)$$

3. Results and Discussion

In order to get the results, Eqs. (12)-(14) with Eqs. (15) and (16) are solved numerically via Keller-box method. The similarity solutions for velocity, temperature and concentration profiles as well as skin friction

coefficient, Nusselt number and Sherwood number are obtained and displayed graphically. The effects of pertinent parameters such as Casson fluid parameter β , magnetic parameter M , porosity parameter K , thermal Grashof number Gr , moving wedge parameter γ , Prandtl number Pr , radiation parameter R_d , Schmidt number Sc and chemical reaction parameter R are graphically displayed and discussed. The accuracy of the present method is assessed through comparison with previously reported results, as displayed in Table 1.

Table 1 reveals the comparison of skin friction coefficient for different values of m with those obtained by Yih [2] and Mukhopadhyay and Mandal [17], and are observed in close agreement.

Table 1 Comparison of friction factor for various values of m for Newtonian Fluid when $M = K = Gr = Gm = R_d = R = \delta = 0$.

		$f''(0)$	
m	Yih [2]	Mukhopadhyay and Mandal [17]	Present results
-0.05	0.213484	0.213802	0.21321
0.0	0.332057	0.332206	0.33206
0.3333	0.757448	0.757586	0.75743
1	1.232588	1.232710	1.23259

Variation of velocity profile for various values of β , M and Gr are displayed in Figs. 2 to 4, respectively. Fig. 2 shows that increasing values of β enhances the fluid velocity and reduces the thickness of the momentum boundary layer. Physically, increase in β reduces the yield stress p_y , and consequently, the thickness of momentum boundary layer decreases. From Fig. 3, it is noted that fluid velocity increases and momentum boundary layer thickness reduces with increase in M . Since magnetic field is the ratio of the electromagnetic force to viscous force that measure the capacity of applied magnetic field. Besides this, the drag offered by porous medium diminishes as the permeability of porous medium rises.

On the other hand, the variation of Gr displayed in Fig. 4 describes that velocity of fluid is higher for large values of Gr . As buoyancy parameter is the only term appears

in momentum equation that coupled the energy equation with the momentum equation. Hence, buoyancy force enhances the influence of temperature field on velocity field will be excited and consequently, the flow being accelerated. In addition, increase in Gr give rise the influence of convection on velocity control.

The variation of the dimensionless temperature profile for various values of Pr and R_d is illustrated in Figs. 5 and 6, respectively. Fig. 5 portrays that dimensionless temperature lower with higher values of Pr . Physically, thermal conductivity reduces due to larger Pr , so the thickness of thermal boundary layer become shortens and temperature falls. Fig. 6 examines that increase in R_d intensifies the dimensionless temperature across the boundary region. Due to the relative contribution of conduction heat transfer to thermal radiation heat transfer, reduction in the thermal resistance of the surface and enhancement in the convective heat transfer to the fluid, the thermal boundary layer becomes thicker with R_d .

The variation of dimensionless concentration profile for different values of Sc and R is exhibited in Figs. 7 and 8, respectively. Fig. 7 demonstrates that fluid concentration drops with increase in Sc . It is worth mentioning here that $Sc < 1$ shows that the momentum diffusivity is smaller than the species diffusivity, while $Sc > 1$ present that the momentum diffusivity exceeds the species diffusivity. Physically, Sc measures the relative importance of viscosity and mass diffusivity. Hence, heavier species with low thermal diffusivity causes a significant reduction in concentration boundary layer thickness. Further, the concentration boundary layer for Hydrogen ($Sc = 0.22$) becomes relatively thicker than Propyl Benzene at 25°C at one atmospheric pressure ($Sc = 2.57$). Fig. 8 reveals that fluid concentration is higher when $R < 0$, whereas observed to be lower when $R > 0$. The reason is that, generative/destructive chemical reaction has a tendency to enhance/reduce diffusion and thereby, an increase/decrease in chemical molecular diffusivity of the species concentration. Consequently, concentration boundary layer becomes thicker/thinner.

In order to get insight the variation of skin

friction coefficient, Nusselt number and Sherwood number for different values of β , M , Gr , K , Gm , γ , R_d , Pr , R and Sc is plotted in Figs. 9 to 12, respectively. Fig. 9 exhibits that increase in β and γ reduces the friction factor, while reverse trend is noticed with M and Gr . Generally, increment in γ exerts the high pressure on the flow; which helps to improve the velocity and temperature fields. It is noted from Fig. 10, that wall shear stress grows with increase in K . Also, the stronger values of M and K has significantly affected the friction factor when $\gamma > 0$. Fig. 11 illustrates that increment in Pr and R_d raises the heat transfer rate effectively when $M > 0$. Finally, Fig. 12 depicts that increment in M , Sc and R causes an enhancement in mass transfer rate. Comparatively, the influence of on Sherwood number is found less pronounced.

4. Conclusion

Some observations from this study are

1. The fluid velocity is observed to be higher with increase in β and M .
2. The influence of M on velocity profile is more pronounced when $K = 0$.
3. The wall shear stress was observed to be more pronounced with increase in γ and K .
4. Nusselt number is excited more when $R_d > 0$ $R_d > 0$.
5. Sherwood number is noticed to be higher when $R > 0$.

Acknowledgement

The authors would like to acknowledge Ministry of Higher Education (MOHE) and Research Management Centre Universiti Teknologi Malaysia (UTM) for the financial support through vot numbers 4F713 and 13H74 for this research.

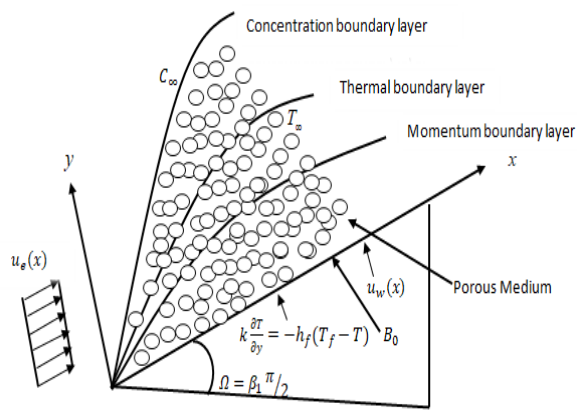


Fig. 1 Physical model and coordinate system

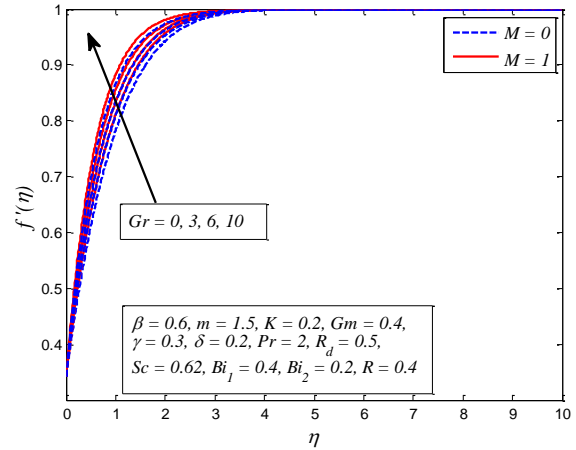


Fig. 4 Variation of Gr on velocity profile for different values of M

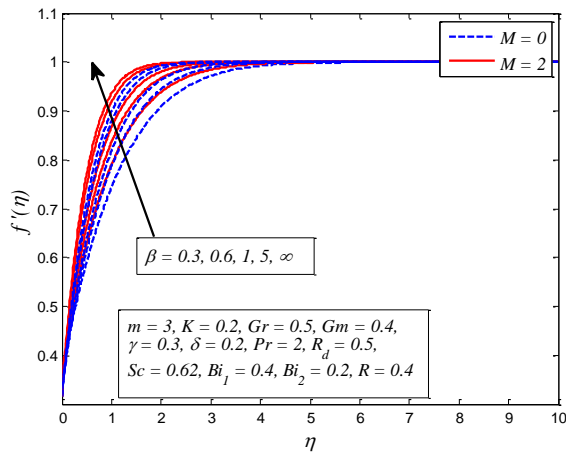


Fig. 2 Variation of β on velocity profile for different values of M

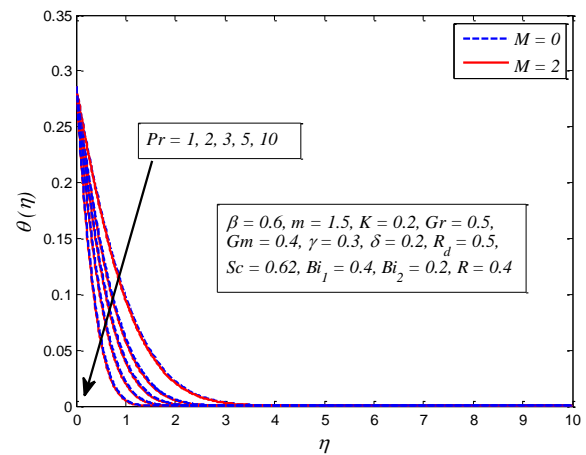


Fig. 5 Variation of Pr on temperature profile for different values of M

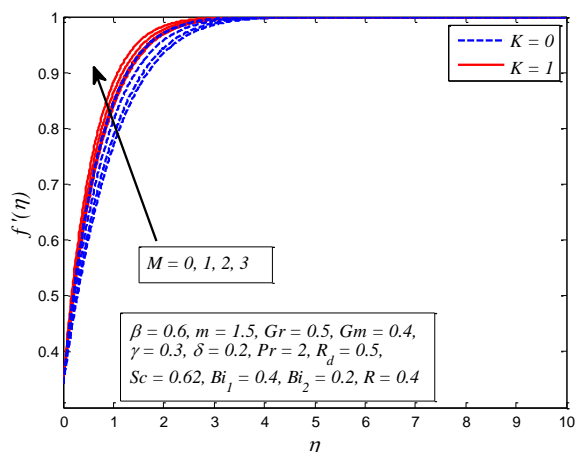


Fig. 3 Variation of M on velocity profile for different values of K

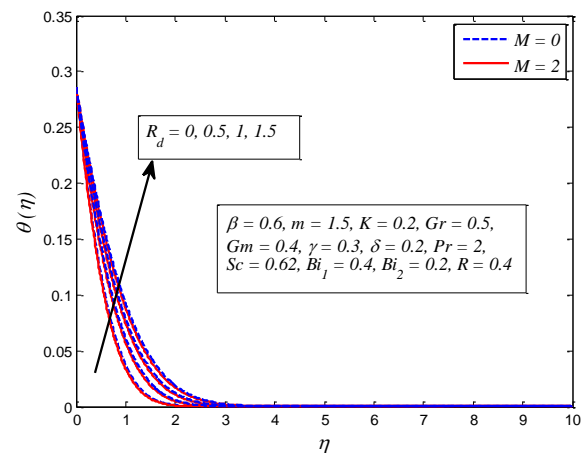


Fig. 6 Variation of R_d on temperature profile for different values of M

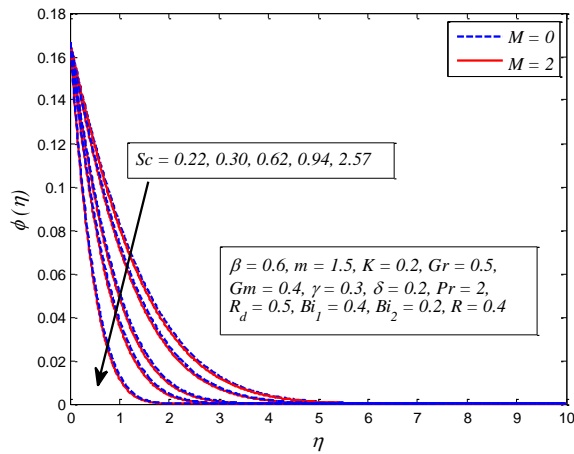


Fig. 7 Variation of Sc on concentration profile for different values of M

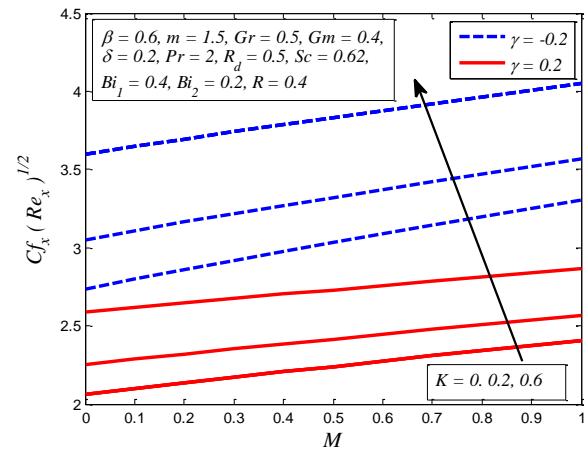


Fig. 10 Variation of skin friction coefficient for different values of K , γ and M

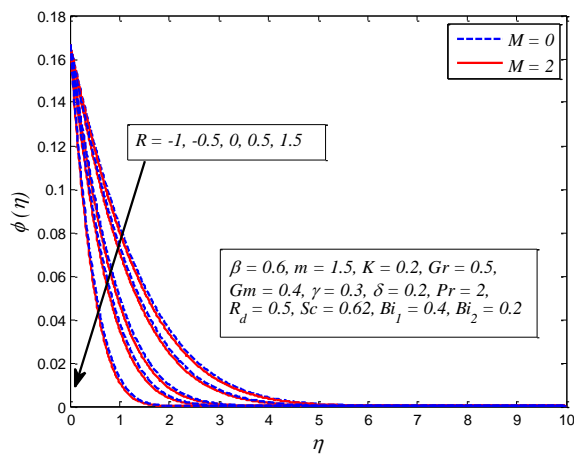


Fig. 8 Variation of R on concentration profile for different values of M .

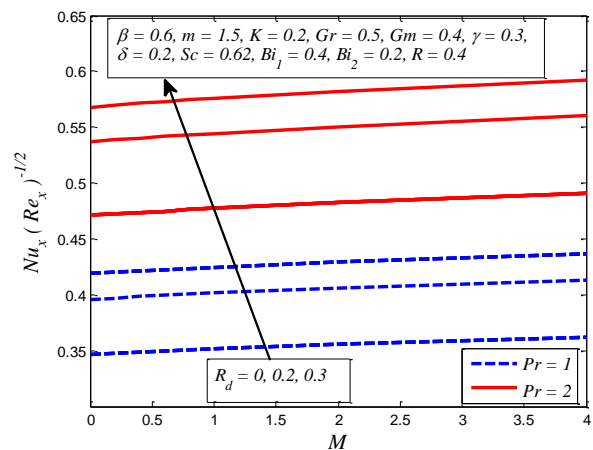


Fig. 11 Variation of Nusselt number for different values of Pr , R_d and M .

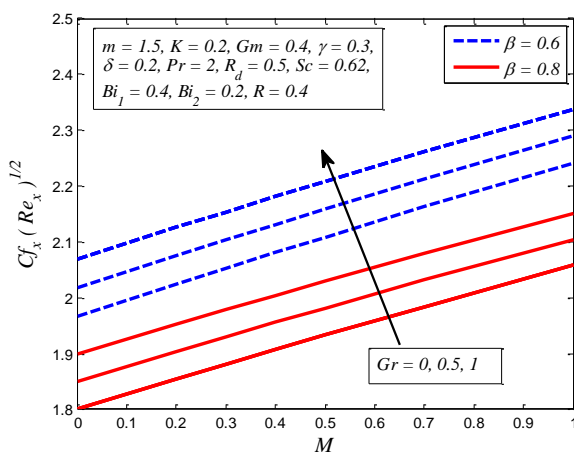


Fig. 9 Variation of skin friction coefficient for different values of β , Gr and M

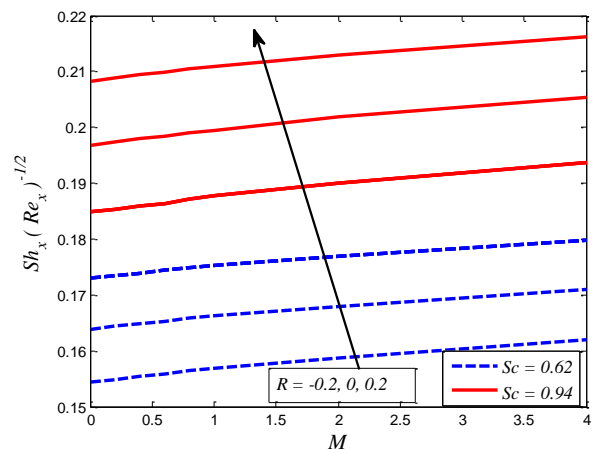


Fig. 12 Variation of Sherwood number for different values of Sc , R and M .

References

- [1] Watanabe, T., Pop, I. (1994) "Thermal boundary layers in magnetohydrodynamic flow over a flat plate in the presence of a transverse magnetic field" in *Acta Mechanica*, Vol. 238. pp 233–238.
- [2] Yih, K.A. (1999) "MHD forced convection flow adjacent to a non-isothermal wedge." in *International Communication in Heat & Mass Transfer*, Vol. 26. pp 819–827.
- [3] Chamkha, A.J., Mujtaba, M., Quadri, A., Issa, C. (2003) "Thermal radiation effects on MHD forced convection flow adjacent to a non-isothermal wedge in the presence of a heat source or sink" in *Heat & Mass Transfer*, Vol. 39. pp. 305–312.
- [4] Ishak, A., Nazar, R., Pop, I. (2009) "MHD boundary-layer flow of a micropolar fluid past a wedge with constant wall heat flux" in *Communication in Nonlinear Science and Numerical Simulation*, Vol.14. pp. 109–118.
- [5] Uddin, Z., Kumar, M. (2013) "Hall and ion-slip effect on MHD boundary layer flow of a micro polar fluid past a wedge" in *Scientia Iranica*, Vol. 20. pp. 467–476.
- [6] Zhang, C., Zheng, L., Zhang, X., Chen, G. (2014) "MHD flow and radiation heat transfer of nanofluids in porous media with variable surface heat flux and chemical reaction" in *Applied Mathematical Modelling*, Vol. 39. pp. 165–181.
- [7] Khan, W.A., Culham, R., Haq, R.U. (2015) "Heat transfer analysis of mhd water functionalized carbon nanotube flow over a static / moving wedge" in *Journal of Nanomaterials*, Vol. 16. No. 1. pp. 112.
- [8] Pandey, A.K., Kumar, M. (2016) "Effect of viscous dissipation and suction/injection on MHD nanofluid flow over a wedge with porous medium and slip" in *Alexandria Engineering Journal*, Vol. 55, pp. 3115–3123.
- [9] Aydin, O., Kaya, A. (2008) "Radiation effect on MHD mixed convection flow about a permeable vertical plate" in *Heat & Mass Transfer*, Vol. 45. pp 239–246.
- [10] Kandasamy, R., Muhaimin, I., Khamis, A.B. (2009) "Thermophoresis and variable viscosity effects on MHD mixed convective heat and mass transfer past a porous wedge in the presence of chemical reaction" in *Heat Mass Transfer*, Vol. 45. PP. 703–712.
- [11] Hsiao, K.L. (2011) "MHD mixed convection for viscoelastic fluid past a porous wedge" in *International Journal of Nonlinear Mechanics*, Vol. 46. pp. 1–8.
- [12] Su, X., Zheng, L., Zhang, X., Zhang, J. (2012) "MHD mixed convective heat transfer over a permeable stretching wedge with thermal radiation and ohmic heating" in *Chemical Engineering Science*, Vol. 78. pp. 1–8.
- [13] Khan. M, Ramzan, A., Azeem, S. (2013) "MHD Falkner-Skan flow with mixed convection and convective boundary conditions" in *Walailak Journal of Science & Technologi*, Vol. 10. pp. 517–529.
- [14] Prasad, K.V., Datti, P.S., Vajravelu, K. (2013) "MHD mixed convection flow over a permeable non-isothermal wedge." in *Journal of King Saud University-Science*, Vol. 25. pp. 313–324.
- [15] Mohammad, S.A. (2014) "Radiation effect on mhd mixed convection flow along an isothermal vertical wedge embedded in a porous medium with heat generation" in *Al-Rafidain Engineering*, Vol. 22. pp. 57–68.
- [16] Ravindran, R., Ganapathirao, M., Pop, I. (2014) "Effects of chemical reaction and heat generation/absorption on unsteady mixed convection MHD flow over a vertical cone with non-uniform slot mass transfer" in *International Journal of Heat & Mass Transfer*, Vol. 73. pp. 743–751.
- [17] Mukhopadhyay, S., Mandal, I.C. (2014) "Boundary layer flow and heat transfer of a Casson fluid past a symmetric porous wedge with surface heat flux" in *Chinese Physics B*, Vol.23. No. 4. pp. 44702.
- [18] Mahanta, G., Shaw, S. (2015) "3D Casson fluid flow past a porous linearly stretching sheet with convective boundary condition" in *Alexandria Engineering Journal*, Vol. 54. pp. 653–659.
- [19] Imtiaz, M., Hayat, T., Alsaedi, A. (2016) "Mixed convection flow of Casson nanofluid over a stretching cylinder with convective boundary conditions." in *Advanced Powder Technology*, Vol. 27. pp. 2245–2256.
- [20] Raju, C.S.K., Sandeep, N. (2016) "Nonlinear radiative magnetohydrodynamic Falkner-Skan flow of Casson over a wedge" in *Alexandria*

Engineering Journal, Vol. 55. pp. 2045–2054.

- [21] Sarif, N.M., Salleh, M.Z., Nazar, R. (2013) “Numerical solution of flow and heat transfer over a stretching sheet with newtonian heating using the keller box method” in *Procedia Engineering*, Vol. 53. pp. 542–554.